

Machine Learning-Enhanced Feasibility Studies on the Production of New Particles with Preferential Couplings to Third Generation Fermions at the LHC

PhD(c). Cristian Fernando Rodríguez Cruz¹
c.rodriguez45@uniandes.edu.co

Research advisors:

Prof. Andrés Florez¹ (ca.florez@uniandes.edu.co)

Prof. J. Jones-Pérez² (jones.j@pucp.edu.pe)

¹Universidad de los Andes

²Pontificia Universidad Católica del Perú

January 26, 2026

Outline

1 Introduction

- Standard Model of Particle Physics
- Deficiencies of the SM
- LHC and Beyond the SM Physics

2 Phenomenological Framework

- Monte-Carlo Pipeline
- Machine Learning in High Energy Physics

3 $U(1)_{T_R^3}$ Model

- Theoretical Deals
- Production Channel
- Search Channel
- Kinematic Variables
- Gradient Boosting

4 U_1 Leptoquark Model

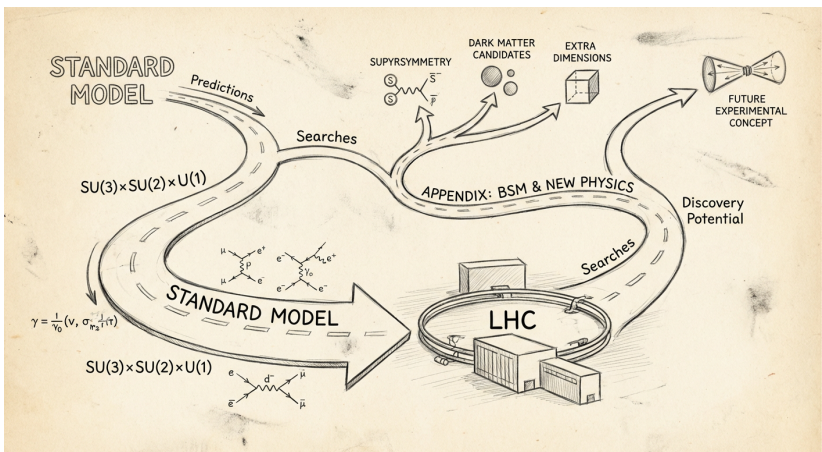
- Single Channels Sensitivity Reach
- Combined Sensitivity Reach

5 Z' Interferences

6 Summary and Conclusions

7 Backup

Introduction



Standard Model of Particle Physics: A Successful Framework

Core Theoretical Structure

- ### • Fermion Sector:

- 3 generations
 - Left-handed doublets:

$$Q_L = \begin{pmatrix} q_u \\ q_d \end{pmatrix}_L ; \quad L_L = \begin{pmatrix} \ell \\ \nu_\ell \end{pmatrix}_L$$

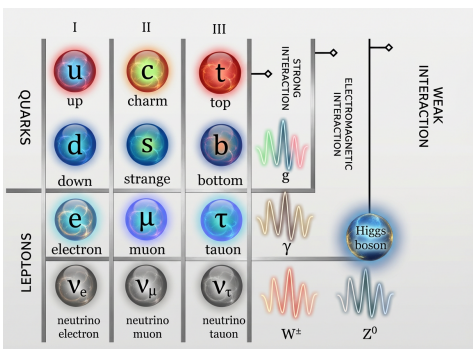
- Right-handed singlets: $q_{uR}, q_{dR}; \ell_R$
 - Flavor structure from CKM mixing
 - Initially, ν_R not required (no mass)

- Gauge Group:

- $SU(3)_C \times SU(2)_L \times U(1)_Y$
 - Strong force: $SU(3)_C$ (QCD)
 - Electroweak: $SU(2)_L \times U(1)_Y$

- Higgs Mechanism:

- $SU(2)_L \times U(1)_Y \rightarrow U(1)_{\text{EM}}$
 - Masses to W^\pm, Z^0 bosons
 - Massless γ
 - Fermion masses via Yukawa couplings
 - Higgs boson h discovered (LHC 2012)



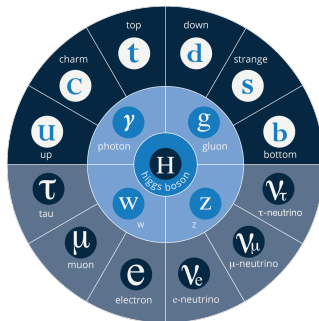
Key Features

- **Particle spectrum:** 12 fermions + 5 bosons
 - **QFT:** Renormalizable, gauge invariant, anomaly-free
 - **Tested experimentally:** Exceptional agreement with data
 - **Predictive power:** Successfully tested at LHC

Deficiencies of the SM

The SM cannot be complete:

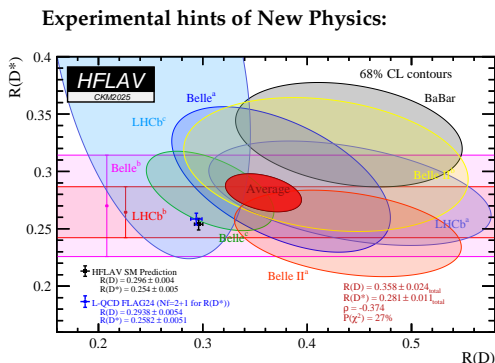
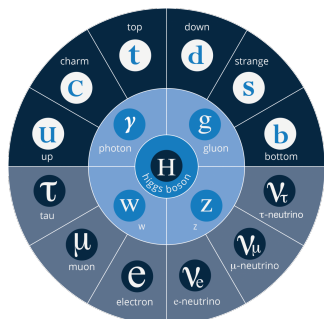
- Unexplained ν masses
 - No explanation for DM
 - Matter-antimatter asymmetry unsolved
 - Gravity not included



Deficiencies of the SM

The SM cannot be complete:

- Unexplained ν masses
 - No explanation for DM
 - Matter-antimatter asymmetry unsolved
 - Gravity not included

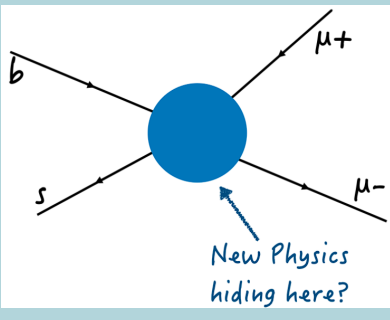


Recent measurements of the $R(D)$ and $R(D^*)$ ratios show a $\sim 3\sigma$ deviation from SM predictions, suggesting possible lepton universality violation.

B-Meson Anomalies

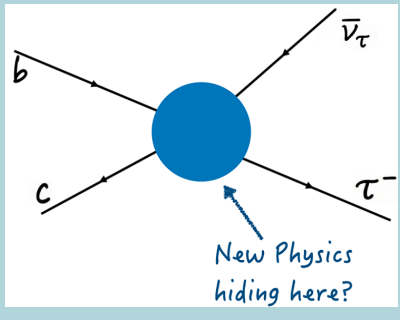
R_K Anomalies

$$R_K = \frac{\mathcal{B}(B \rightarrow K\mu^+\mu^-)}{\mathcal{B}(B \rightarrow Ke^+e^-)}$$



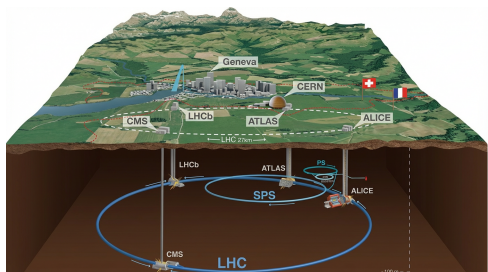
R_D Anomalies

$$R_D = \frac{\mathcal{B}(B \rightarrow D\tau\nu)}{\mathcal{B}(B \rightarrow D\ell\nu)}$$



- The B-meson anomalies hint at lepton flavor universality violation.
 - NP coupled mainly to 3G-fermions address these anomalies.
 - Currently, R_K is SM-compatible, tensions in R_D still persist.

The Large Hadron Collider (LHC)



LHC Physics Program

- SM parameter determinations
 - Precision Tests
 - Direct searches for BSM physics
 - Cross sections & Decay rates measurements
 - Angular Correlations, among others

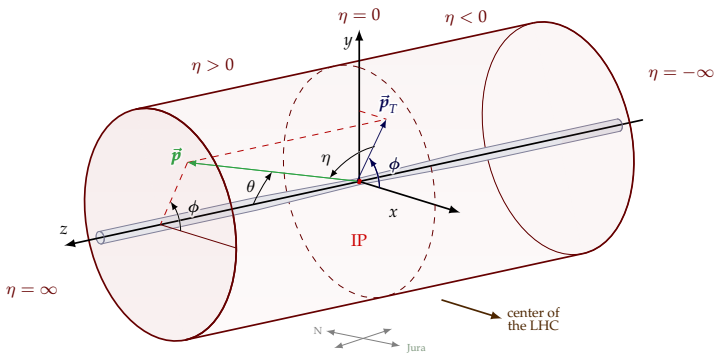
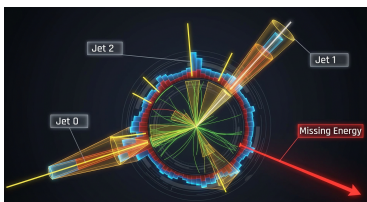
World's largest particle collider:

- Located at CERN, at the France-Switzerland border
 - 27 km circumference ring
 - Designed to probe the TeV scale
 - Four main experiments:
ATLAS, CMS, LHCb, ALICE
 - pp collisions at $\sqrt{s} = 13.6$ TeV
 - Bunches of $\sim 10^{11}$ Particles
 - 40 MHz collision rate
 - Small beam spot size
 - Run-II Luminosity $\sim 150 \text{ fb}^{-1}$
 - RUN-III currently on analysis
with $\sim 300 \text{ fb}^{-1}$
 - High luminosity upgrade
(HL-LHC) planned for 2029

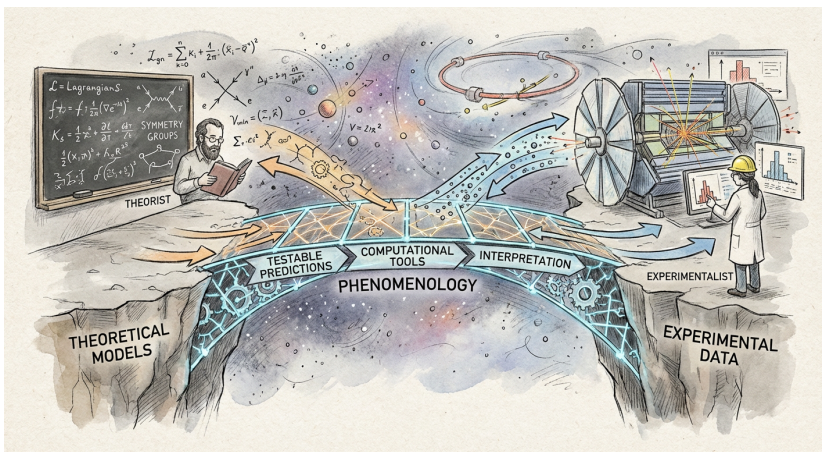
Collider Observables

Collider Kinematics

$$\left\{ \begin{array}{l} \text{Pseudorapidity: } \eta = -\ln \tan(\theta/2) \\ \text{Transverse momentum: } p_T = p \sin(\theta) \\ \text{Azimuthal angle: } \phi \\ \text{Deposited energy: } E \end{array} \right.$$



Phenomenological Framework



From Theory to Simulation: FeynRules



Input: .fr Model File

- Lagrangian \mathcal{L} terms
 - Particle definitions: F, V, S fields
 - Gauge symmetries: $SU(N)$, $U(1)$
 - Parameters: masses, couplings
 - Mixing matrices, constraints
 - Output: UFO model files

Madgraph-Pythia-Delphes

Ecosystem for Event Simulation

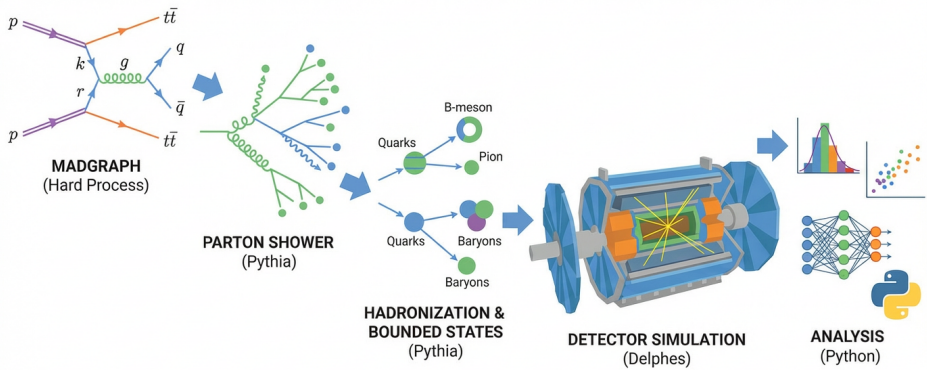
Goal: Produce realistic simulated data comparable to experimental observations

Input: BSM model in UFO format, collider setup, process definitions, parameters

Pipeline: UFO model → LHE (parton) → HEPMC (hadron) → ROOT (detector)

Output: Simulated events in ROOT format, ready for physics analysis

Automated: Cross-sections, widths, branching ratios calculated automatically



Statistical Significance

Statistical Significance

It is the parametric test

$$\kappa = \frac{\langle t \rangle_B - \langle t \rangle_{S+B}}{\sigma_{S+B}}$$

where $t \sim \chi^2$ is the optimal test.

Event Yield

The event yield in each bin is $N_i = \sigma_i \cdot \mathcal{L} \cdot \epsilon_i$, where:

- σ_i : cross section
 - \mathcal{L} : integrated luminosity
 - ϵ_i : selection efficiency

The significance becomes:

$$\kappa = \frac{\sum_i \sigma_{s_i} \epsilon_{s_i} w_i}{\sqrt{\sum_i (\sigma_{s_i} \epsilon_{s_i} + \sigma_{b_i} \epsilon_{b_i} + \delta_{\text{sys}}^2) w_i^2}} \sqrt{\mathcal{L}} \quad (1)$$

Strategies to improve κ :

- Increase luminosity \mathcal{L}
 - Optimize cuts to enhance ϵ_s/ϵ_b
 - Increase σ_s via higher \sqrt{s} for heavier states
 - Use multivariate discriminants (BDT, DNN)
 - Reduce systematic uncertainties δ_{sys}
 - Exploit correlations between bins

Machine Learning Revolution in HEP

Why ML in Particle Physics?

- **High-dimensional data:**
Complex detector outputs
 - **Complex patterns:**
Jet and event classification
 - **Rare signals:**
Need optimal background rejection
 - **Automation:**
Reduce manual feature engineering
 - **Computational efficiency:**
Speed up workflows

Traditional vs ML Approaches

Traditional:

- Manual cut-based analysis
 - Simple kinematic variables
 - Univariate methods
 - Limited feature engineering

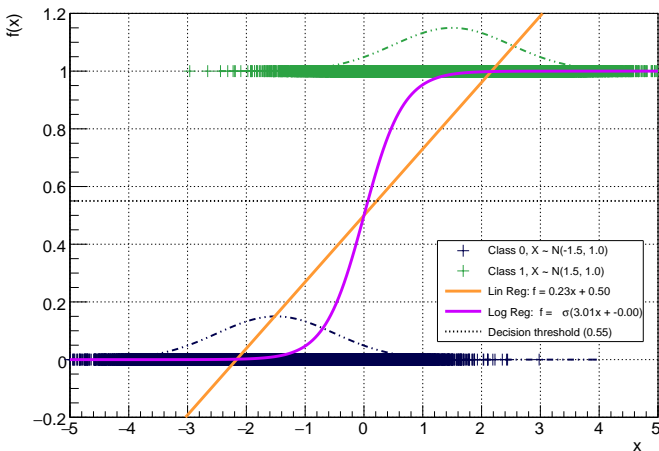
Machine Learning:

- Multivariate classifiers (BDT, NN)
 - Deep learning on raw data
 - Anomaly detection for BSM searches

Typical Current Applications

- **Event classification:** Signal/background separation
 - **Jet tagging:** $b/c/\tau$ -jet identification
 - **Object reconstruction:** Particle flow, tracking
 - **Anomaly detection:** Model-agnostic BSM searches
 - **Simulation acceleration:** Fast calorimeter simulation

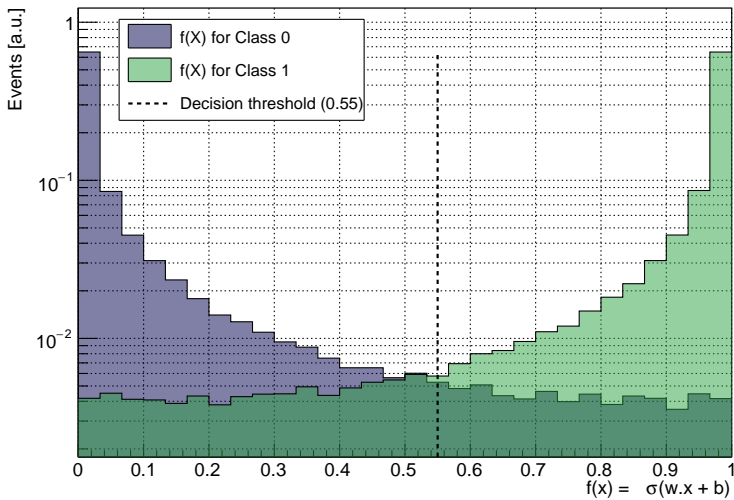
How does the binary classifier work?



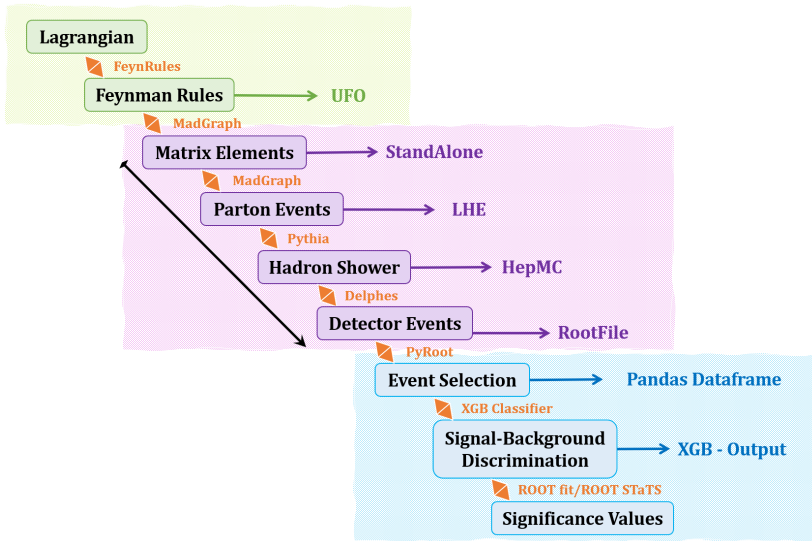
Be aware: The real performance is the same for both algorithms in terms of classification accuracy. The difference lies in interpretability and probabilistic output.

A New Distribution Emerges

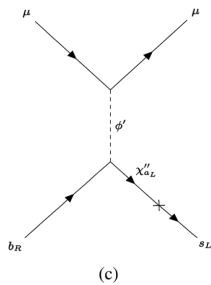
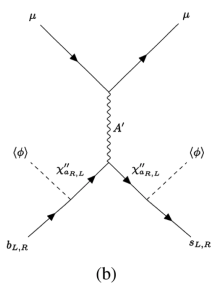
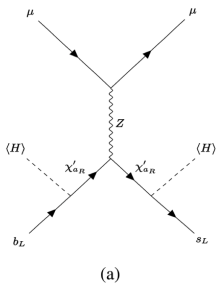
Distribution of $f(x) = \sigma(w \cdot x + b)$



Feasibility Studies Workflow



$U(1)_{T_R^3}$ Model



Deeper Origin of Hypercharge?

SM Electric Charge Formula

In the SM, electric charge emerges from electroweak symmetry breaking

$$Q_{\text{EM}} = T_L^3 + \frac{\gamma}{2}$$

where T_L^3 is weak isospin ($SU(2)_L$) and Y is hypercharge ($U(1)_Y$)

Could Υ emerge from additional gauge symmetries?

Pati-Salam tries to restore left-right symmetry:

$$Y = 2T_R^3 + \frac{B - L}{2}$$

$$Q_{\text{EM}} = T_L^3 + T_R^3 + \frac{B - L}{4}$$

This induce challenges: Anomaly cancellation, Higgs sector, mass scales, fermion masses, among others.

Key Question

Can hypercharge be explained by a more fundamental gauge structure?

This could provide a deeper understanding of the SM's chiral fermion assignments.

Need of modify Higgs Mechanism

SM fermion masses from Yukawa couplings

The SM yukawa couplings are not invariant under the new symmetry

$$\mathcal{L}_{\text{Yukawa}} = \underbrace{-y_e \bar{L}_L \Phi e_R}_{\text{Lepton Yukawa}} + \underbrace{-y_d \bar{Q}_L \Phi d_R}_{\text{Down quark Yukawa}} + \underbrace{-y_u \bar{Q}_L \tilde{\Phi} u_R}_{\text{Up quark Yukawa}} + \text{h.c.} \quad (2)$$

The SM masses arise after EWSB when $\langle \Phi \rangle = v_h/\sqrt{2} \implies m_f = \frac{1}{\sqrt{2}} y_f v_h$

Need of modify Higgs Mechanism

SM fermion masses from Yukawa couplings

The SM yukawa couplings are not invariant under the new symmetry

$$\mathcal{L}_{\text{Yukawa}} = \underbrace{-y_e \bar{L}_L \Phi e_R}_{\text{Lepton Yukawa}} + \underbrace{-y_d \bar{Q}_L \Phi d_R}_{\text{Down quark Yukawa}} + \underbrace{-y_u \bar{Q}_L \tilde{\Phi} u_R}_{\text{Up quark Yukawa}} + \text{h.c.} \quad (2)$$

The SM masses arise after EWSB when $\langle \Phi \rangle = v_h/\sqrt{2} \implies m_f = \frac{1}{\sqrt{2}} y_f v_h$

However, if we add the $U(1)_{T_p^3}$ charges to the SM fields as

Field	$SU(3)_C$	$SU(2)_L$	$U(1)_Y$	$U(1)_{T_R^3}$
q_L	3	2	$1/6$	0
ℓ_L	1	2	$-1/2$	0
u_R^c	3	1	$-2/3$	$-1/2$
d_R^c	3	1	$1/3$	$1/2$
ℓ_R^c	1	1	1	$1/2$

We get $\gamma_u = \gamma_d = \gamma_e = 0$ is mandatory \implies **No Masses, Chiral anomalies also arise.**

Mass mechanism in the $U(1)_{T_p^3}$ Model

Modifications to the Scalar and Fermion Sectors

- We need two scalar fields:
 - The usual Higgs doublet H , with $\langle H \rangle = v_h/\sqrt{2}$.
 - A new complex scalar singlet ϕ , with $\langle \phi \rangle = v_\phi/\sqrt{2}$.
 in order to decouple the energy scales of $U(1)_{T_R^3}$ and $SU(2)_L \times U(1)_Y$ breaking
 - Fermions acquire mass from the mixture with a new vector-like fermion χ_f .
 - Right-handed neutrinos ν_R are added to cancel anomalies in the lepton sector.

The terms in the Lagrangian density that contribute to the mass of physical fermions are:

$$-\mathcal{L} \supset Y_{f_L} \bar{f}'_L \chi'_{fR} H + Y_{f_R} \bar{\chi}'_{fL} f'_R \phi^* + m_{\chi'_f} \bar{\chi}'_{fL} \chi'_{fR} + \text{h.c.} \quad (3)$$

Therefore, in the vacuum, the mass matrix for each fermion f is given by

$$M_f = \begin{pmatrix} 0 & Y_{f_L} v_h / \sqrt{2} \\ Y_{f_R} v_\phi / \sqrt{2} & m_{\chi'_f} \end{pmatrix}, \quad \Rightarrow \quad \begin{cases} m_f m_{\chi_f} = \frac{Y_{f_L} v_h Y_{f_R} v_\phi}{2} \\ m_f^2 + m_{\chi_f}^2 = m_{\chi'_f}^2 + \frac{1}{2} \left(Y_{f_L}^2 v_h^2 + Y_{f_R}^2 v_\phi^2 \right), \end{cases} \quad (4)$$

The masses will rise from diagonalizing this matrix.

Mass mechanism in the $U(1)_{T_p^3}$ Model

Modifications to the Scalar and Fermion Sectors

- We need two scalar fields:
 - The usual Higgs doublet H , with $\langle H \rangle = v_h/\sqrt{2}$.
 - A new complex scalar singlet ϕ , with $\langle \phi \rangle = v_\phi/\sqrt{2}$.
 in order to decouple the energy scales of $U(1)_{T_R^3}$ and $SU(2)_L \times U(1)_Y$ breaking
 - Fermions acquire mass from the mixture with a new vector-like fermion χ_f .
 - Right-handed neutrinos ν_R are added to cancel anomalies in the lepton sector.

After spontaneous symmetry breaking

$$H = \left(\frac{1}{\sqrt{2}} (v_h + \rho_0 + iG_0) \right), \quad \phi = \frac{1}{\sqrt{2}} (v_\phi + \rho_\phi + iG_\phi), \quad (3)$$

where G^\pm, G^0 are the Goldstone bosons eaten by W^\pm and Z^0 , and G_ϕ is the Goldstone boson eaten by the new Z' /dark photon.

While the scalar parts ρ_0 and ρ_ϕ mix to get the physical mass eigenstates h and ϕ ,

$$M_{\text{scalar}}^2 = \begin{pmatrix} 2\lambda_H v_h^2 & \lambda_{H\phi} v_h v_\phi \\ \lambda_{H\phi} v_h v_\phi & 2\lambda_\phi v_\phi^2 \end{pmatrix} \implies \begin{cases} m_h^2 - m_{\phi'}^2 = \sqrt{(4\lambda_{H\phi}^2 v_h^2 v_\phi^2) + (\lambda_H v_h^2 - \lambda_\phi v_\phi^2)^2} \\ m_h^2 + m_{\phi'}^2 = \lambda_H v_h^2 + \lambda_\phi v_\phi^2 \end{cases} \quad (4)$$

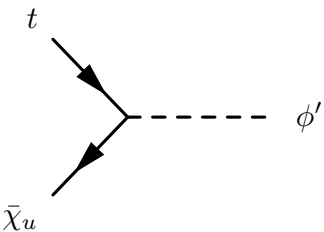
New Yukawa Interactions

The Yukawa interactions of the physical fermions with the scalar bosons have the form

$$-\mathcal{L}_{\text{yuk}} = h \bar{\psi}_{f_L} \gamma_h \psi_{f_R} + \phi' \bar{\psi}_{f_L} \gamma_\phi \psi_{f_R}, \quad (5)$$

with $\psi_f = (f, \chi_f)^T$, and $\mathcal{Y}_{f_L R}$ are 2×2 yukawa masses after rotation to the mass basis.

So, you have new vertex like



that converts a SM fermion to a heavy vector-like fermion via the emission of a ϕ' boson...

New Yukawa Interactions

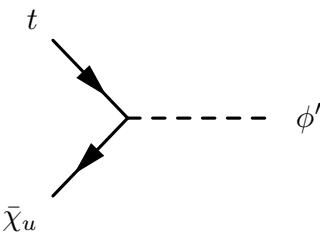
The Yukawa interactions of the physical fermions with the scalar bosons have the form

$$-\mathcal{L}_{\text{yuk}} = h \bar{\psi}_{f_L} \mathcal{Y}_h \psi_{f_R} + \phi' \bar{\psi}_{f_L} \mathcal{Y}_{\phi'} \psi_{f_R}, \quad (5)$$

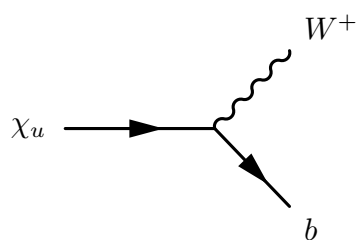
with $\psi_f = (f, \chi_f)^T$, and $\mathcal{Y}_{f_L, R}$ are 2×2 yukawa masses after rotation to the mass basis.

So, you have new vertex like

... in addition to the vertex

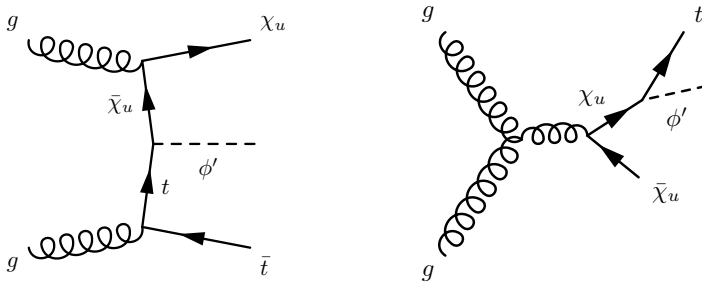


that converts a SM fermion to a heavy vector-like fermion via the emission of a ϕ' boson...



that involves a top-like quark decay via the emission of a W boson.

Production Channel



Production Cross Section

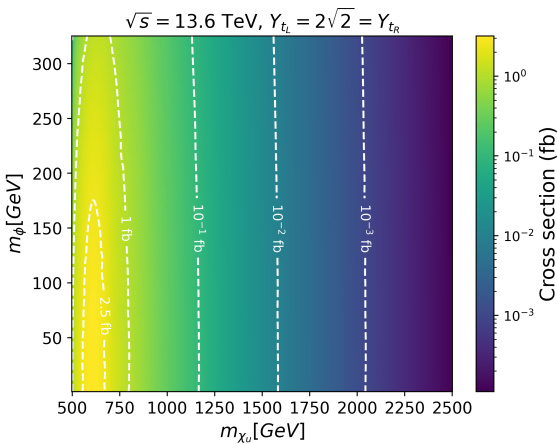
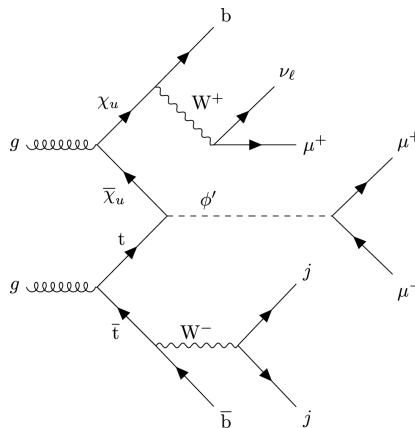


Fig.: Projected cross section (fb) plot for $pp \rightarrow t\chi_u \phi'$ and subsequent decay as a function of $m(\chi_u)$ and $m(\phi')$.

Feasible Experimental Signatures

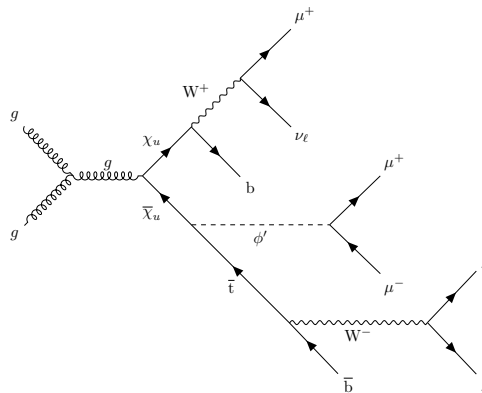
Representative Feynman diagram for the production of a ϕ' boson in association with a χ_u vector-like quark through the fusion of a top quark and χ_u vector-like quark.



The ϕ' decays to a pair of muons, the top quark decays fully hadronically, and the χ_u decays semi-leptonically to muons, neutrinos and b -jets.

Feasible Experimental Signatures

Representative Feynman diagram for the production of a ϕ' boson in association with a χ_u vector-like quark through the fusion of a gluon pair from incoming protons.

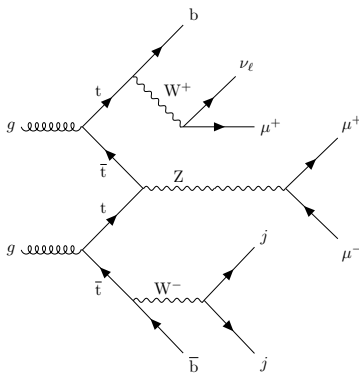


The ϕ' decays to a pair of muons, the top quark that decays fully hadronically, and the χ_u decay semi-leptonically to muons, neutrinos and jets.

Feasible Experimental Signatures

Background

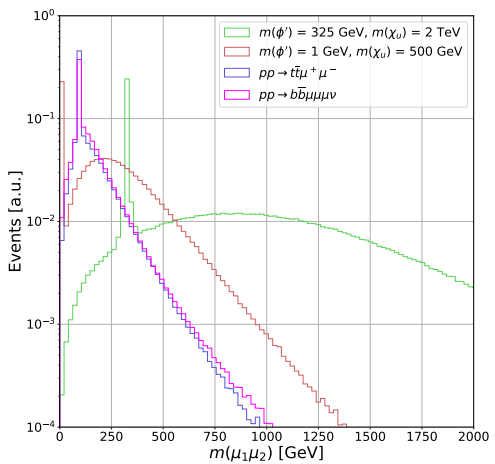
Representative Feynman diagram for a background event. A Z boson is produced in association with a top quark through the fusion of a top, anti top pair from incoming protons.



The Z boson subsequently decays to a pair of muons and the two spectator top quarks decay semi-leptonically and purely hadronically to muons, neutrinos and jets, resulting in the same final states as the signal event.

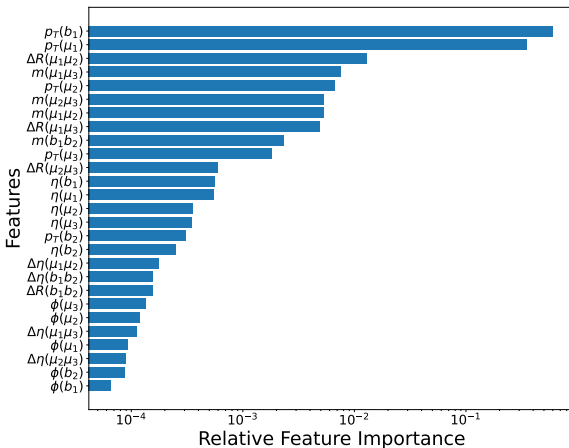
Feasible Experimental Signatures

Kinematic Variables



Invariant mass distribution of the transverse momentum. The ground processes and two signal

Feature Importance



- Benchmark signal scenario with $m(\phi') = 325 \text{ GeV}$ and $m(\chi_u) = 2000 \text{ GeV}$.
- Main Features: boosted μ_1 and b_1 jet, angular correlated muons and resonant ϕ' decay.

Optimal Discriminant Output

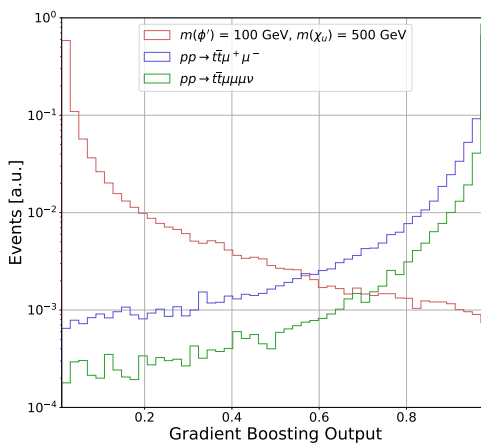


Fig: Output of the gradient boosting algorithm for a benchmark $m(\phi') = 100$ GeV and $m(\chi_u) = 500$ GeV signal, and dominant backgrounds. The distributions are normalized to unity.

Signal Significance

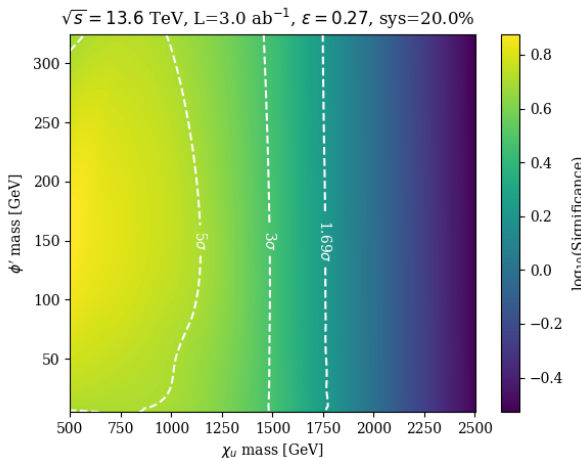


Fig.: Signal significance for the high luminosity LHC era, considering with 3000 fb^{-1} of collected data.

Eur. Phys. J. C (2025) 85:379
<https://doi.org/10.1140/epjc/s10052-025-14085-1>

THE EUROPEAN
PHYSICAL JOURNAL C



Regular Article - Theoretical Physics

Probing light scalars and vector-like quarks at the high-luminosity LHC

U. S. Qureshi^{1,a} , A. Gurrola^{1,b} , A. Flórez^{2,c} , C. Rodríguez^{2,d}

¹ Department of Physics and Astronomy, Vanderbilt University, Nashville, TN, USA

² Physics Department, Universidad de los Andes, Bogotá, Colombia

Received: 30 October 2024 / Accepted: 15 March 2025

© The Author(s) 2025

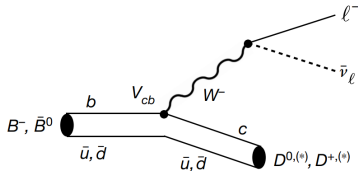
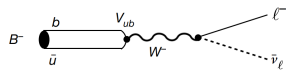
U_1 Leptoquark Model

$R(D)$ and $R(D^*)$ anomalies

Flavor Observables

$$R(D) = \frac{\text{BR}(B \rightarrow D\tau\nu)}{\text{BR}(B \rightarrow D\ell_{(e,\mu)}\nu)}, \quad R(D^{(*)}) = \frac{\text{BR}(B \rightarrow D^{(*)}\tau\nu)}{\text{BR}(B \rightarrow D^{(*)}\ell_{(e,\mu)}\nu)}$$

Standard Model (Tree-level)



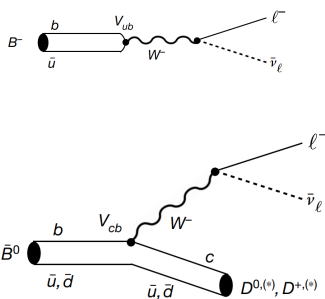
$B^- \rightarrow D^0 \ell^- \bar{\nu}_\ell$ via W^- exchange

R(D) and R(D) anomalies*

Flavor Observables

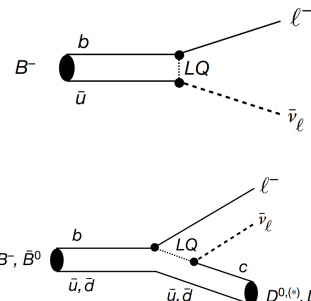
$$R(D) = \frac{\text{BR}(B \rightarrow D\tau\nu)}{\text{BR}(B \rightarrow D\ell_{(e,\mu)}\nu)}, \quad R(D^{(*)}) = \frac{\text{BR}(B \rightarrow D^{(*)}\tau\nu)}{\text{BR}(B \rightarrow D^{(*)}\ell_{(e,\mu)}\nu)}$$

Standard Model (Tree-level)



$B^- \rightarrow D^0 \ell^- \bar{\nu}_\ell$ via W^- exchange

Leptoquark Mediated



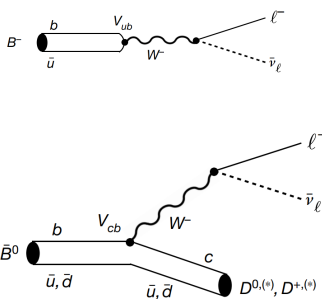
$B^- \rightarrow D^0 \ell^- \bar{\nu}_\ell$ via leptoquark exchange

R(D) and R(D) anomalies*

Flavor Observables

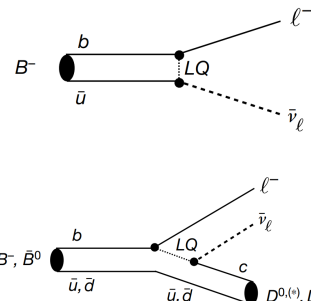
$$R(D) = \frac{\text{BR}(B \rightarrow D\tau\nu)}{\text{BR}(B \rightarrow D\ell_{(e,\mu)}\nu)}, \quad R(D^{(*)}) = \frac{\text{BR}(B \rightarrow D^{(*)}\tau\nu)}{\text{BR}(B \rightarrow D^{(*)}\ell_{(e,\mu)}\nu)}$$

Standard Model (Tree-level)



$B^- \rightarrow D^0 \ell^- \bar{\nu}_\ell$ via W^- exchange

Leptoquark Mediated



$B^- \rightarrow D^0 \ell^- \bar{\nu}_\ell$ via leptoquark exchange

How can we test this hypothesis?

The vector leptoquark U_1 model

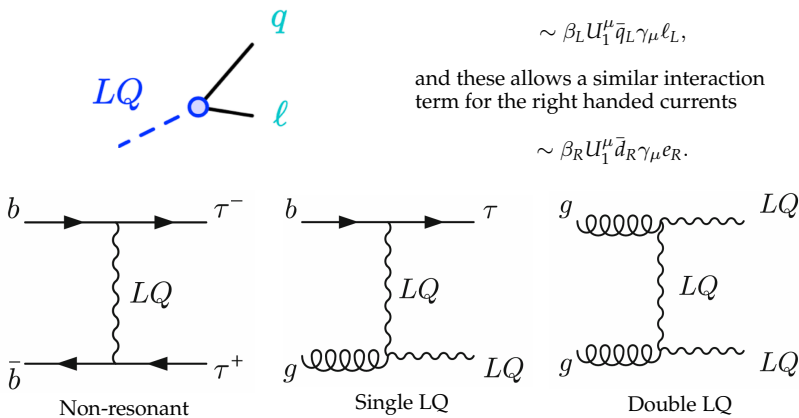
A leptoquark is defined as a particle with a vertex that mix vectors and quarks.

If U_1 is a vector leptoquark that preserves the chirality on the vertex, we expect an interaction term like

$$\sim \beta_L U_1^\mu \bar{q}_L \gamma_\mu \ell_L,$$

and these allows a similar interaction term for the right handed currents

$$\sim \beta_R U_1^\mu \bar{d}_R \gamma_\mu e_R$$



Where the SM charges for the leptoquark, in the $Y = 2(Q - T_3)$ convention, are

	\bar{q}_L	ℓ_L^j	$\bar{q}_L \gamma_\mu \ell_L$	U_1^μ
$U(1)$	-1/3	-1	-4/3	+4/3
SU(2)	2	2	1	1
SU(3)	3	1	3	3

Then, the leptoquark $U_1 \sim (\mathbf{3}_C, \mathbf{1}_I, 4/3_Y)$.

Where the SM charges for the leptoquark, in the $Y = 2(Q - T_3)$ convention, are

	\bar{q}_L	ℓ_L^j	$\bar{q}_L \gamma_\mu \ell_L$	U_1^μ
$U(1)$	-1/3	-1	-4/3	+4/3
SU(2)	2	2	1	1
SU(3)	3	1	3	3

Then, the leptoquark $U_1 \sim (\mathbf{3}_C, \mathbf{1}_I, 4/3_Y)$.

The full Lagrangian for the vector leptoquark is

$$\begin{aligned} \mathcal{L}_U = & -\frac{1}{2} U_{\mu\nu}^\dagger U^{\mu\nu} + M_U^2 U_\mu^\dagger U^\mu - i g_s U_\mu^\dagger T^a U_\nu G_a^{\mu\nu} - \frac{2i}{3} g' U_\mu^\dagger U_\nu B^{\mu\nu} \\ & + \frac{g_u}{\sqrt{2}} \left[U_1^\mu \left(\beta_L^{ij} \bar{q}_L^i \gamma_\mu e_L^j + \beta_R^{ij} \bar{d}_R^i \gamma_\mu e_R^j \right) + \text{h.c.} \right] \end{aligned}$$

where $U_{\mu\nu} = \mathcal{D}_\mu U_\nu - \mathcal{D}_\nu U_\mu$, $\mathcal{D}_\mu = \partial_\mu - i g_s G_\mu^a T^a - i \frac{2}{3} g_Y B_\mu$, and the couplings β_L and β_R are complex 3×3 matrices in flavor space.

Where the SM charges for the leptoquark, in the $Y = 2(Q - T_3)$ convention, are

	\bar{q}_L	ℓ_L^j	$\bar{q}_L \gamma_\mu \ell_L$	U_1^μ
$U(1)$	$-1/3$	-1	$-4/3$	$+4/3$
SU(2)	$\bar{\mathbf{2}}$	$\mathbf{2}$	$\mathbf{1}$	$\mathbf{1}$
SU(3)	$\bar{\mathbf{3}}$	$\mathbf{1}$	$\bar{\mathbf{3}}$	$\mathbf{3}$

Then, the leptoquark $U_1 \sim (\mathbf{3}_C, \mathbf{1}_I, 4/3_Y)$.

The full Lagrangian for the vector leptoquark is

$$\begin{aligned} \mathcal{L}_U = & -\frac{1}{2} U_{\mu\nu}^\dagger U^{\mu\nu} + M_U^2 U_\mu^\dagger U^\mu - i g_s U_\mu^\dagger T^a U_\nu G_a^{\mu\nu} - \frac{2i}{3} g' U_\mu^\dagger U_\nu B^{\mu\nu} \\ & + \frac{g_u}{\sqrt{2}} \left[U_1^\mu \left(\beta_L^{ij} \bar{q}_L^i \gamma_\mu e_L^j + \beta_R^{ij} \bar{d}_R^i \gamma_\mu e_R^j \right) + \text{h.c.} \right] \end{aligned}$$

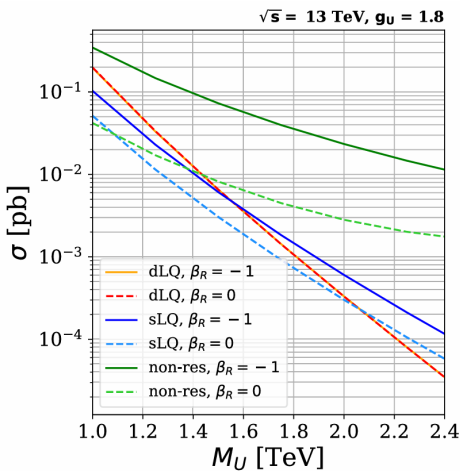
where $U_{\mu\nu} = \mathcal{D}_\mu U_\nu - \mathcal{D}_\nu U_\mu$, $\mathcal{D}_\mu = \partial_\mu - i g_s G_\mu^a T^a - i \frac{2}{3} g_Y B_\mu$, and the couplings β_L and β_R are complex 3×3 matrices in flavor space.

Constraints from $\Delta F = 2$ and lepton flavor violation impose a hierarchy with dominant third generation couplings:

$$|\beta_L^{11}|, |\beta_L^{12}|, |\beta_L^{21}|, |\beta_L^{22}|, |\beta_L^{31}| \ll |\beta_L^{13}| \ll |\beta_L^{23}|, |\beta_L^{32}| \ll |\beta_R^{33}|, |\beta_L^{33}| = \mathcal{O}(1), \quad (6)$$

where β_R is diagonal.

Leptoquark Production Mechanisms at 13 TeV



Production Channels

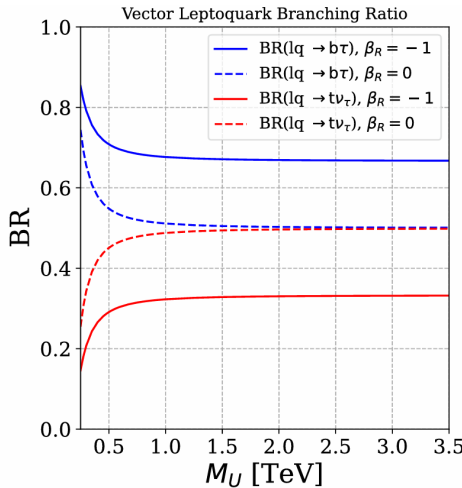
- **dLQ:** Pair production
QCD-mediated
 β_R independent
 - **sLQ:** Single production
 β_R sensitive
 $\times 2$ enhancement
 - **non-res:** Non-resonant
 β_R sensitive
 $\times 10$ enhancement

Cross-over Point

$\sigma_{\text{sLQ}} > \sigma_{\text{dLQ}}$ for $M_{\text{LQ}} \gtrsim 1.5$ TeV
(exact value depends on g_W)

Leptoquark Branching Fractions

Branching Ratios vs. β_R Parameter



Main Decay Channels

- LQ $\rightarrow b\tau$: Dominant
Primary for $R(D^{(*)})$ anomalies
 - LQ $\rightarrow t\nu_\tau$: Competing
Affects total width
 - LO $\rightarrow c\tau, s\nu_\tau$: Subdominant

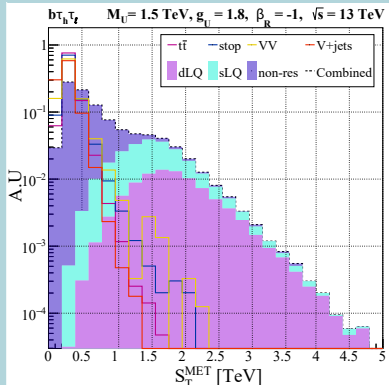
β_R Dependence

Controls right-handed
couplings:

- $\beta_R = 0$: Pure left-handed
 - $\beta_R > 0$: Mixed chirality
 - Affects collider signatures

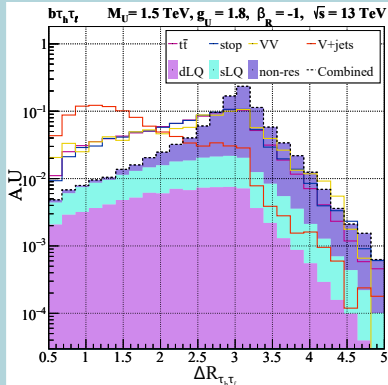
S_T^{MeT} observable

$$S_T^{\text{MeT}} = \text{MeT} + \sum_i |p_T^i|$$



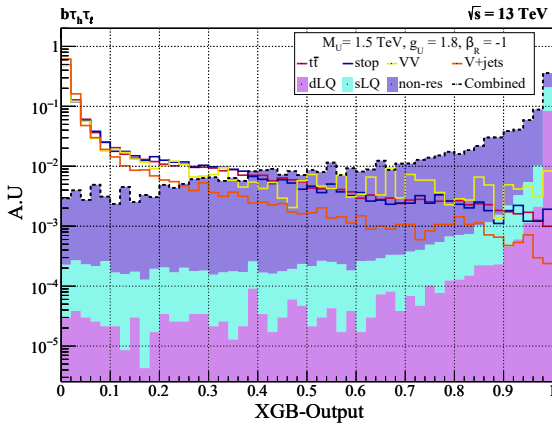
ΔR Separation

$$\Delta R = \sqrt{\Delta\eta^2 + \Delta\phi^2}$$



- Separation of sLQ and dLQ with the backgrounds enhanced via S_T^{MeT} , a measure of the boostedness of the event.
 - Separation of non-resonant production with the backgrounds enhanced via ΔR between the τ candidates.

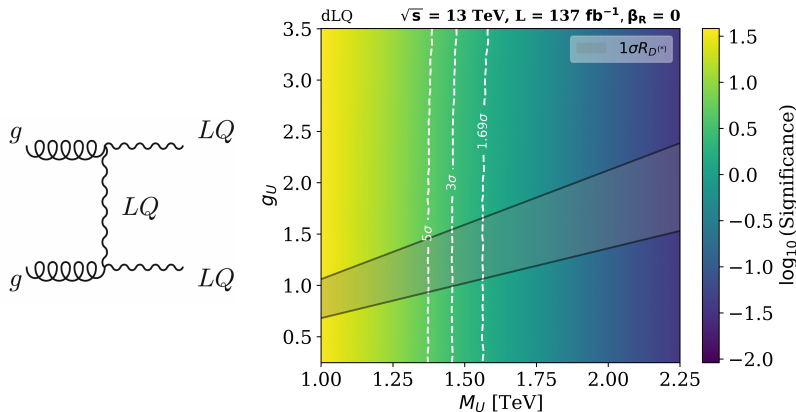
XGB-output



- We can evaluate a score for the signal and background events using the discriminator algorithm.
 - Each production channel has contributions in each one of the six detection channels.

Double Leptoquark Production

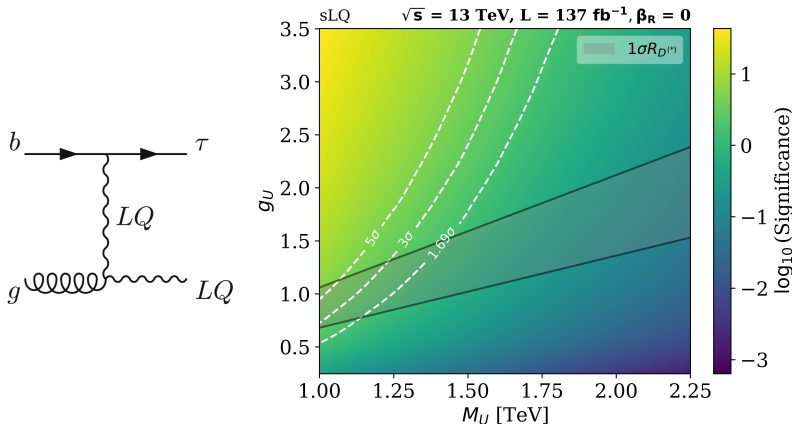
The Sensitivity Reach / only left-handed currents



- dLQ production depends only on α_{QCD} and the available energy.
 - So, the potential reach is independent of the global coupling with fermions g_u .

Single leptoquark production

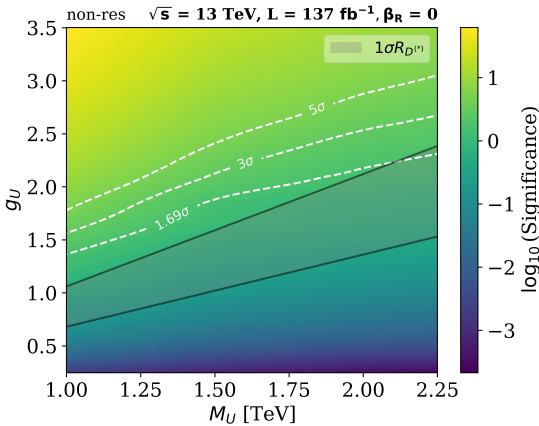
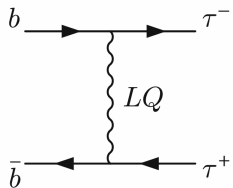
The Sensitivity Reach / only left-handed currents



- Single leptoquark production is sensitive to both, mass and couplings.
 - It contributes to the regions of high coupling constants at higher masses than double leptoquark production.

Non-resonant Production

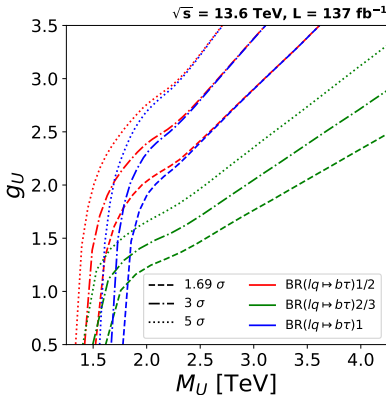
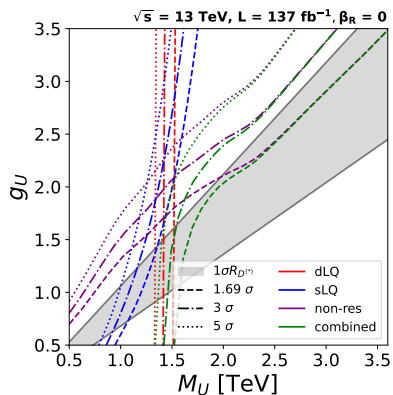
The Sensitivity Reach / only left-handed currents



- Non-resonant production is highly dependent on the couplings, so it dominates the regions of high coupling constants at all masses.

Combined Sensitivity Reach

Combined Sensitivity Reach

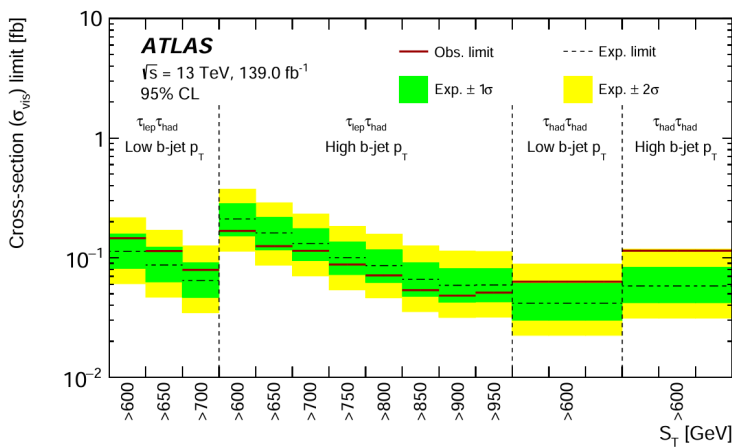


- A combined analysis of the three production channels suggests better sensitivity for high coupling constants.
 - Depending on the benchmark β_L, β_R values, the branching ratio to $b\tau$ can vary, affecting the sensitivity reach.

Combined Sensitivity Reach

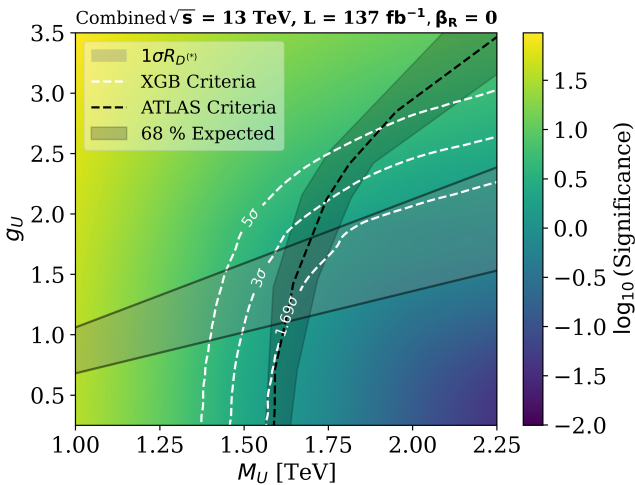
ATLAS Results

Left-handed currents only



- In parallel ATLAS released a search following a similar approach [ArXiv:2305.15962].

Combined Sensitivity Reach

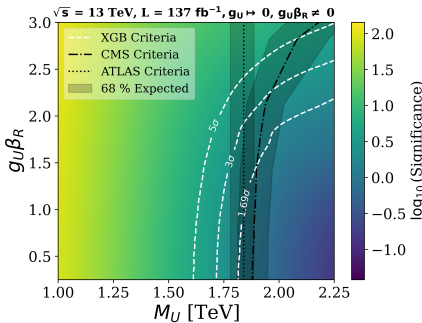
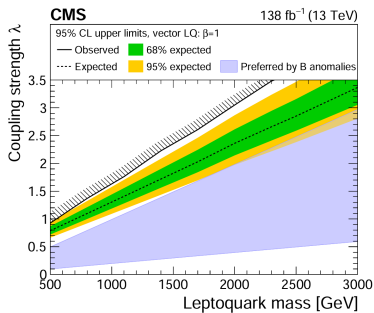


- Our ML-based analysis suggests better sensitivity for high coupling constants.

Combined Sensitivity Reach

Combined Sensitivity Reach

The Sensitivity Reach / only right-handed currents



The case $BR(lq \rightarrow b\tau) = 1$ corresponds to the only right-handed currents coupling. The sensitivity compared with the latest one from the CMS [2308.07826] and ATLAS Collaborations [2303.01294], again we suggest better sensitivity for high coupling constants.

Z' Interferences

The need of a Z' boson in gauge U_1 models

If U_1 has a gauge origin, we could rewrite the interaction term in the covariant derivative as

$$\psi_L^{\text{SM}} = \begin{pmatrix} q_{Lr} \\ q_{Lg} \\ q_{Lb} \\ \ell_L \end{pmatrix} \implies \mathcal{L}_{\text{int}} \sim U_{1\alpha}^\mu \bar{\psi}_L^{\text{SM}} \gamma_\mu T_+^\alpha \psi_L^{\text{SM}} + \text{h.c.}, \quad T_+^\alpha = \begin{pmatrix} 0 & 0 & 0 & \delta_{r\alpha} \\ 0 & 0 & 0 & \delta_{g\alpha} \\ 0 & 0 & 0 & \delta_{b\alpha} \\ 0 & 0 & 0 & 0 \end{pmatrix},$$

we have six generators T_{\pm}^{α} with closure relation and projecting into a color singlet operator:

$$\sum_{\alpha} [T_+^{\alpha}, T_-^{\alpha}] = 3T_{B-L} = \begin{pmatrix} 1 & 0 & 0 & 0 \\ 0 & 1 & 0 & 0 \\ 0 & 0 & 1 & 0 \\ 0 & 0 & 0 & -3 \end{pmatrix}.$$

So, the gauge group with this leptoquark must include a $U(1)_{B-L}$ symmetry (The right-handed currents also have a similar interaction term).

The need of a Z' boson in gauge U_1 models

If U_1 has a gauge origin, we could rewrite the interaction term in the covariant derivative as

$$\psi_L^{\text{SM}} = \begin{pmatrix} q_{Lr} \\ q_{Lg} \\ q_{Lb} \\ \ell_L \end{pmatrix} \implies \mathcal{L}_{\text{int}} \sim U_{1\alpha}^\mu \bar{\psi}_L^{\text{SM}} \gamma_\mu T_+^\alpha \psi_L^{\text{SM}} + \text{h.c.}, \quad T_+^\alpha = \begin{pmatrix} 0 & 0 & 0 & \delta_{r\alpha} \\ 0 & 0 & 0 & \delta_{g\alpha} \\ 0 & 0 & 0 & \delta_{b\alpha} \\ 0 & 0 & 0 & 0 \end{pmatrix},$$

we have six generators T_{\pm}^{α} with closure relation and projecting into a color singlet operator:

$$\sum_{\alpha} [T_+^{\alpha}, T_-^{\alpha}] = 3T_{B-L} = \begin{pmatrix} 1 & 0 & 0 & 0 \\ 0 & 1 & 0 & 0 \\ 0 & 0 & 1 & 0 \\ 0 & 0 & 0 & -3 \end{pmatrix}.$$

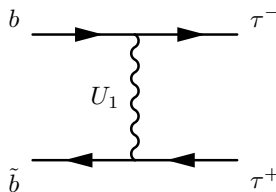
So, the gauge group with this leptoquark must include a $U(1)_{B-L}$ symmetry (The right-handed currents also have a similar interaction term).

The interaction terms for the Z' boson have the form

$$\begin{aligned}\mathcal{L}_{\text{int}} &\sim Z'_\mu \left(\bar{\psi}_L^{\text{SM}} \gamma^\mu (3T_{B-L}) \psi_L^{\text{SM}} \right) \\ &\sim Z'_\mu \left(\bar{q}_L \gamma^\mu q_L - 3 \bar{\ell}_L \gamma^\mu \ell_L \right).\end{aligned}$$

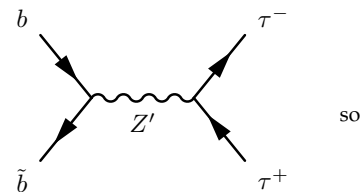
Interference with a Z' vector boson

Non-Resonant Production (leptoquarks) Resonant Production (neutral bosons)



$$\mathcal{M}_{U_1} \sim \frac{1}{t - m_{ll_L}^2 + im_{U_1}\Gamma_{U_1}}, \quad (7)$$

the interference has the form

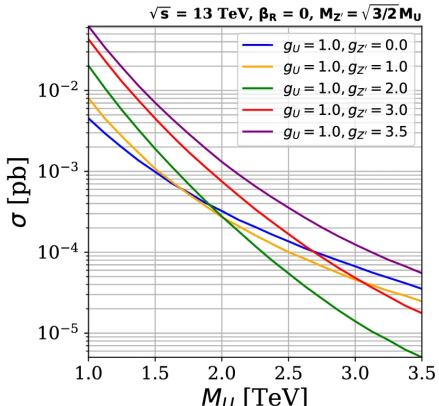
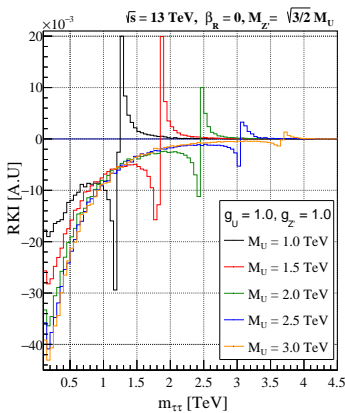


$$\mathcal{M}_{Z'} \sim \frac{1}{s - m_{Z'}^2 + im_{Z'}\Gamma_{Z'}}, \quad (8)$$

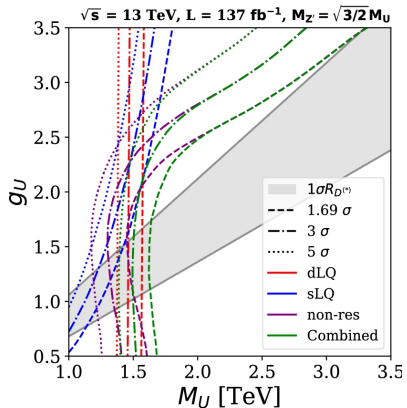
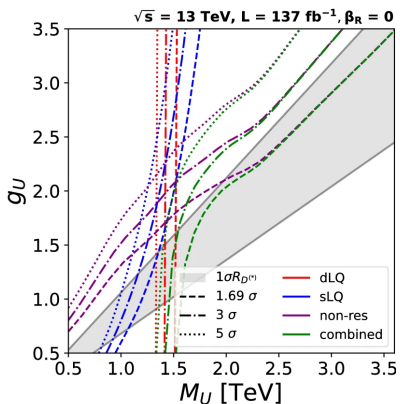
$$dm \left[-L_{Q+Z}^{\prime }-\left(-L_Q^{\prime }-L_Z^{\prime }\right) \right] \quad s\quad \left[(t-m_{LQ}^2)^2+m_{LQ}^2\Gamma _{LQ}^2\right] \left[(s-m_{Z'}^2)^2+m_{Z'}^2\Gamma _{Z'}^2\right]$$

Similary for Polarized final states.

Interference with a Z' vector boson



Effects on the Sensitivity reach





On the sensitivity reach of LQ production with preferential couplings to third generation fermions at the LHC

A. Flórez^{1,a} , J. Jones-Pérez^{2,b} , A. Gurrola^{3,c}, C. Rodríguez^{1,d} , J. Peñuela-Parra^{1,e}

¹ Departamento de Física, Universidad de Los Andes, Cra. 1 # 18a-12, Bogotá, Colombia

² Sección Física, Departamento de Ciencias, Pontificia Universidad Católica del Perú, Apartado 1761, Lima, Peru

³ Department of Physics and Astronomy, Vanderbilt University, Nashville, TN 37235, USA

Received: 31 July 2023 / Accepted: 22 October 2023
© The Author(s) 2023

Summary and Conclusions

Related Research Projects

Feasibility to probe the dynamical scotogenic model at the LHC

Gustavo Ardila-Tafurth,^{*} Andrés Flórez,[†] Cristian Rodríguez,[‡] and Maud Sarazin[§]
Departamento de Física, Universidad de los Andes, Bogotá 111711, Colombia

Óscar Zapata

*Instituto de Física, Universidad de Antioquia, Calle 70 # 52-21
Apartado Aéreo 1226, Medellín, Colombia*

(Dated: December 22, 2025)

Related Research Projects

Feasibility to probe the dynamical scotogenic model at the LHC

Gustavo Ardila-Tarthur^{*}, Andrés Flórez[†], Cristian Rodríguez[‡] and Maud Sarazin[§]
Departamento de Física, Universidad de los Andes, Bogotá 111711, Colombia

Óscar Zapata

*Instituto de Física, Universidad de Antioquia, Calle 70 # 52-21
Apartado Aéreo 1226, Medellín, Colombia*

(Dated: December 22, 2025)

On BSM Signatures in Ditau Channels at the LHC

A. Flórez,* C. Rodriguez,† J. Reyes,‡ and AC. Parra§

*Departamento de Física, Universidad de Los Andes,
Cra. 1 # 18a-12, Bogotá, Colombia*

J. Jones-Pérez

*Sección Física, Departamento de Ciencias,
Pontificia Universidad Católica del Perú,
Apartado 1761, Lima, Peru
(Dated: Upcoming)*

Future explorations

- We will explore the neutrino sector in the $U(1)_{T_R^3}$ model, including possible connections to dark matter, through an intensive study of the parameter space.
 - Extended study of the $R(D)$, $R(D^*)$ anomalies in the context of the $U(1)_{T_R^3}$ model including right-handed neutrinos.
 - We have been exploring models with new scalar doublets and singlets that expose an alternative hypothesis for toponium-like pseudoscalar resonance observed at the LHC.
 -

Thank you for your attention!

Backup Slides

What Do We Look For at the LHC?

Three Complementary Approaches

- **SM Parameter Determination**

- Precisely measure fundamental SM parameters
- Test consistency of the SM framework
- Reduce theoretical uncertainties

- **Indirect Searches (Precision Tests)**

- Measure SM processes with high precision
- Look for deviations in predicted distributions
- Constrain new physics through virtual effects

- **Direct Searches**

- Look for new particles in final states (resonances, excesses)
- Examples: SUSY particles, Z' , leptoquarks, dark matter mediators

Key Types of Measurements

Direct Signatures:

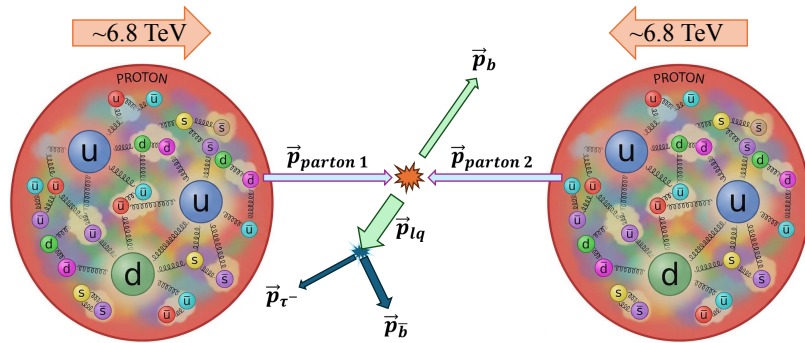
- Resonant mass peaks
- Excess events over SM background
- Missing transverse energy (MET)
- Unusual kinematic features

Precision Observables:

- Differential cross sections
- Angular correlations
- Rare decay rates
- Lepton flavor universality ratios
- Charge-parity (CP) asymmetries

The Quark-Gluon Sea

Partons are the fundamental constituents inside protons: valence quarks (uud) and a **sea** of virtual quark-antiquark pairs and gluons.



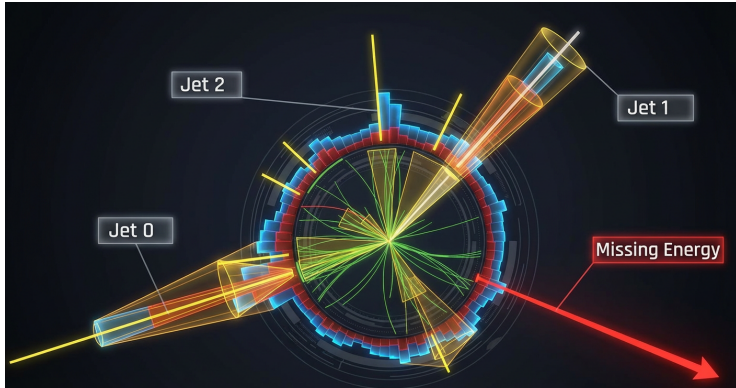
The interacting partons are typically **sea quarks or gluons**, which carry only a fraction of the proton's momentum but dominate the cross-section at high energies.

Jet Clustering & Missing Transverse Momentum

Jet clustering groups collimated particle showers into jets to reconstruct the original quarks/gluons from the hard scatter.

Missing p_T appears as transverse momentum imbalance, signaling undetected particles like neutrinos:

$$\vec{p}_T^{\text{miss}} = - \sum_{\text{visible prods}} \vec{p}_T$$



From Theory to Simulation: FeynRules



Input: .fr Model File

- Lagrangian \mathcal{L} terms
- Particle definitions: F, V, S fields
- Gauge symmetries: $SU(N)$, $U(1)$
- Parameters: masses, couplings
- Mixing matrices, constraints

Output: UFO Format

- Complete Feynman rules (vertices)
- Lorentz and color structures
- Parameter definitions
- Ready to simulate

Features

- ↗ Standardized UFO format
- ↗ Flexible for BSM models
- ↗ Community-driven
- ↘ NLO complexity
- ↘ Poor debugging
- ↘ Performance issues

Why Simulate New Physics Models?

- **Predict signals** for experimental searches
- **Test theoretical consistency** (unitarity, constraints)
- **Optimize analyses** before data collection
- **Interpret potential discoveries** from LHC data
- **Compare predictions** across different models

Statistical Significance

The statistical significance for discovery is a parametric test defined as:

$$\kappa = \frac{\langle t \rangle_B - \langle t \rangle_{S+B}}{\sigma_{S+B}} \quad (9)$$

where $t = -2 \ln[\mathcal{L}(n|S + B)/\mathcal{L}(n|B)] \sim \chi^2$ is the optimal test statistic.

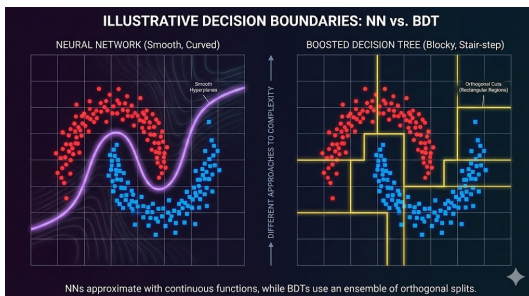
We denote \mathcal{L} as the likelihood for Poisson-distributed event counts n in each bin and gaussian systematic uncertainties.

For binned data analysis, this simplifies to:

$$\kappa = \frac{\sum_i s_i w_i}{\sqrt{\sum_i (s_i + b_i + \delta_{\text{sys}}^2) w_i^2}} \quad (10)$$

where s_i, b_i are signal/background events in bin i , $w_i \sim \ln(1 + s_i/b_i)$ are optimal weights, and δ_{sys} is the systematic uncertainty.

Boosted Decision Trees vs Neural Networks



BDTs

Strengths:

- **Interpretable:** Feature importance rankings
- **Robust:** Handle missing data well
- **Fast training:** Efficient on tabular data
- **Low hyperparameter tuning:** Reasonable defaults work

Limitations:

- **Extrapolation:** Poor outside training range
- **High-dimensional:** Can struggle with many features
- **Discontinuous:** Piecewise constant predictions

Deep NNs

Strengths:

- **Flexible:** Can learn complex non-linearities
- **High-dimensional:** Excel with many features
- **Continuous:** Smooth function approximations
- **Transfer learning:** Pretrained models possible

Limitations:

- **Black box:** Difficult to interpret
- **Data hungry:** Need large training sets
- **Computational:** Require GPUs for large networks
- **Sensitive:** Require careful hyperparameter tuning

HEP Use Cases

BDTs: Preferred for $\sim 10 - 100$ features

NNs: Preferred for low-level data (images, graphs)

Feasible Experimental Signatures

Kinematic Variables

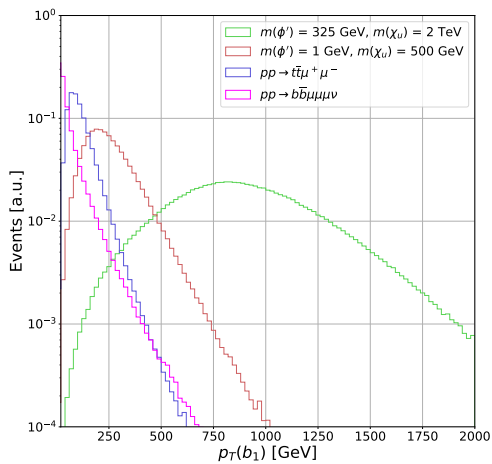


Fig.: Transverse momentum distribution of the leading b-quark jet candidate. The distributions are shown for the two main SM background processes and two signal benchmark points.

Feasible Experimental Signatures

Kinematic Variables

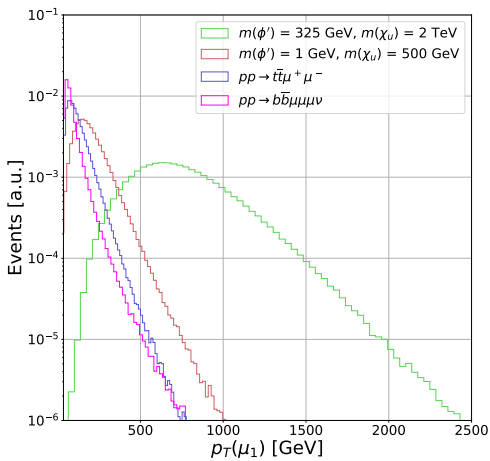


Fig.: Transverse momentum distribution of the leading muon candidate. The distributions are shown for the two main SM background processes and two signal benchmark points.

Where the SM charges for the leptoquark, in the $Y = 2(Q - T_3)$ convention, are

	\bar{q}_L	ℓ_L^j	$\bar{q}_L \gamma_\mu \ell_L$	U_1^μ
$U(1)$	$-1/3$	-1	$-4/3$	$+4/3$
$SU(2)$	$\bar{\mathbf{2}}$	$\mathbf{2}$	$\mathbf{1}$	$\mathbf{1}$
$SU(3)$	$\bar{\mathbf{3}}$	$\mathbf{1}$	$\mathbf{3}$	$\mathbf{3}$

Then, the leptoquark $U_1 \sim (\mathbf{3}_C, \mathbf{1}_I, 4/3_Y)$.

Where the SM charges for the leptoquark, in the $Y = 2(Q - T_3)$ convention, are

	\bar{q}_L	ℓ_L^j	$\bar{q}_L \gamma_\mu \ell_L$	U_1^μ
$U(1)$	$-1/3$	-1	$-4/3$	$+4/3$
$SU(2)$	$\bar{\mathbf{2}}$	$\mathbf{2}$	$\mathbf{1}$	$\mathbf{1}$
$SU(3)$	$\bar{\mathbf{3}}$	$\mathbf{1}$	$\mathbf{3}$	$\mathbf{3}$

Then, the leptoquark $U_1 \sim (\mathbf{3}_C, \mathbf{1}_I, 4/3_Y)$.

The full Lagrangian for the vector leptoquark is

$$\begin{aligned} \mathcal{L}_U = & -\frac{1}{2} U_{\mu\nu}^\dagger U^{\mu\nu} + M_U^2 U_\mu^\dagger U^\mu - i g_s U_\mu^\dagger T^a U_\nu G_a^{\mu\nu} - \frac{2i}{3} g' U_\mu^\dagger U_\nu B^{\mu\nu} \\ & + \frac{g_U}{\sqrt{2}} \left[U_1^\mu \left(\beta_L^{ij} \bar{q}_L^i \gamma_\mu e_L^j + \beta_R^{ij} \bar{d}_R^i \gamma_\mu e_R^j \right) + \text{h.c.} \right] \end{aligned}$$

where $U_{\mu\nu} = \mathcal{D}_\mu U_\nu - \mathcal{D}_\nu U_\mu$, $\mathcal{D}_\mu = \partial_\mu - i g_s G_\mu^a T^a - i \frac{2}{3} g_Y B_\mu$, and the couplings β_L and β_R are complex 3×3 matrices in flavor space.

Where the SM charges for the leptoquark, in the $Y = 2(Q - T_3)$ convention, are

	\bar{q}_L	ℓ_L^j	$\bar{q}_L \gamma_\mu \ell_L$	U_1^μ
$U(1)$	$-1/3$	-1	$-4/3$	$+4/3$
$SU(2)$	$\bar{\mathbf{2}}$	$\mathbf{2}$	$\mathbf{1}$	$\mathbf{1}$
$SU(3)$	$\bar{\mathbf{3}}$	$\mathbf{1}$	$\mathbf{3}$	$\mathbf{3}$

Then, the leptoquark $U_1 \sim (\mathbf{3}_C, \mathbf{1}_I, 4/3_Y)$.

The full Lagrangian for the vector leptoquark is

$$\begin{aligned} \mathcal{L}_U = & -\frac{1}{2} U_{\mu\nu}^\dagger U^{\mu\nu} + M_U^2 U_\mu^\dagger U^\mu - i g_s U_\mu^\dagger T^a U_\nu G_a^{\mu\nu} - \frac{2i}{3} g' U_\mu^\dagger U_\nu B^{\mu\nu} \\ & + \frac{g_u}{\sqrt{2}} \left[U_1^\mu \left(\beta_L^{ij} \bar{q}_L^i \gamma_\mu e_L^j + \beta_R^{ij} \bar{d}_R^i \gamma_\mu e_R^j \right) + \text{h.c.} \right] \end{aligned}$$

where $U_{\mu\nu} = \mathcal{D}_\mu U_\nu - \mathcal{D}_\nu U_\mu$, $\mathcal{D}_\mu = \partial_\mu - i g_s G_\mu^a T^a - i \frac{2}{3} g_Y B_\mu$, and the couplings β_L and β_R are complex 3×3 matrices in flavor space.

Constraints from $\Delta F = 2$ and lepton flavor violation impose a hierarchy with dominant third generation couplings:

$$|\beta_L^{11}|, |\beta_L^{12}|, |\beta_L^{21}|, |\beta_L^{22}|, |\beta_L^{31}| \ll |\beta_L^{13}| \ll |\beta_L^{23}|, |\beta_L^{32}| \ll |\beta_R^{33}|, |\beta_L^{33}| = \mathcal{O}(1), \quad (11)$$

where β_R is diagonal.

Two body scattering

CM-Frame

Consider the process

$$A(\vec{p}_1) + B(\vec{p}_2) \longrightarrow C(\vec{p}_3) + D(\vec{p}_4), \quad (12)$$



From the Golden Rule, the cross section is given by

$$\sigma = \frac{n! (2\pi)^4}{4\sqrt{(\vec{p}_1 \cdot \vec{p}_2)^2 - (m_1 m_2)^2}} \int |\mathcal{M}|^2 \delta^{(4)}(p_1 + p_2 - p_3 - p_4) \frac{d^3 \vec{p}_3}{(2\pi)^3 2E_3} \frac{d^3 \vec{p}_4}{(2\pi)^3 2E_4}. \quad (13)$$

But, in the CM frame, $\vec{p}_1 + \vec{p}_2 = 0$, where

$$\sqrt{(\vec{p}_1 \cdot \vec{p}_2)^2 - (m_1 m_2)^2} = E_1 E_2 |\vec{p}_1|, \quad (14)$$

$$\delta^{(4)}(p_1 + p_2 - p_3 - p_4) = \delta(E_1 + E_2 - E_3 - E_4) \delta^{(3)}(\vec{p}_3 + \vec{p}_4). \quad (15)$$

Thus

$$\sigma = \left(\frac{1}{8\pi}\right)^2 \frac{n!}{(E_1 E_2) |\vec{p}_1|} \int |\mathcal{M}|^2 \frac{\delta\left(E_1 + E_2 - \sqrt{\vec{p}_3^2 + m_3^2} - \sqrt{\vec{p}_4^2 + m_4^2}\right)}{\sqrt{\vec{p}_3^2 + m_3^2} \sqrt{\vec{p}_4^2 + m_4^2}} d\vec{p}_3 \quad (16)$$

Integrating over the radial part $|\vec{p}_3|$, we get

$$\sigma = \left(\frac{1}{8\pi}\right)^2 \frac{n! |\vec{p}_3|}{(E_1 + E_2)^2 |\vec{p}_1|} \int |\mathcal{M}|^2 d\Omega, \quad (17)$$

with

$$|\vec{p}_3| = \frac{1}{2} \frac{\sqrt{((E_1 + E_2)^2 - m_3^2 - m_4^2)^2 - 4m_3^2 m_4^2}}{E_1 + E_2}, \quad (18)$$

the outgoing momentum in the CM frame.

We prefer work with differential cross section as

$$\frac{d\sigma}{d\Omega} = \frac{1}{64\pi^2} \frac{n!}{(E_1 + E_2)^2} \frac{|\vec{p}_3|}{|\vec{p}_1|} |\mathcal{M}|^2. \quad (19)$$

Defining $\sqrt{s} = E_1 + E_2$, we have

$$|\vec{p}_3| = \frac{1}{2} \frac{\sqrt{(s - m_3^2 - m_4^2)^2 - 4m_3^2 m_4^2}}{\sqrt{s}}, \quad |\vec{p}_1| = \frac{1}{2} \frac{\sqrt{(s - m_1^2 - m_2^2)^2 - 4m_1^2 m_2^2}}{\sqrt{s}}. \quad (20)$$

so the differential cross section is

$$\frac{d\sigma}{d\Omega} = \frac{1}{64\pi^2} \frac{n!}{s} \sqrt{\frac{(s - (m_3 + m_4)^2)(s - (m_3 - m_4)^2)}{(s - (m_1 + m_2)^2)(s - (m_1 - m_2)^2)}} |\mathcal{M}|^2. \quad (21)$$

Note that at this point, we don't need to know the explicit form of the matrix element \mathcal{M} , so it is a generic result.

Writting t in terms of s and θ

In general, there are three Lorentz-invariant useful kinematical variables to describe the scattering process, known as Mandelstam variables:

$$\hat{s} = (p_1 + p_2)^2 = (p_3 + p_4)^2 = m_1^2 + m_2^2 + 2p_1^\mu p_{2\mu} = m_3^2 + m_4^2 + 2p_3^\mu p_{4\mu}, \quad (22)$$

$$\hat{t} = (p_1 - p_3)^2 = (p_2 - p_4)^2 = m_1^2 + m_3^2 - 2p_1^\mu p_{3\mu} = m_2^2 + m_4^2 - 2p_2^\mu p_{4\mu}, \quad (23)$$

$$\hat{u} = (p_1 - p_4)^2 = (p_2 - p_3)^2 = m_1^2 + m_4^2 - 2p_1^\mu p_{4\mu} = m_2^2 + m_3^2 - 2p_2^\mu p_{3\mu}. \quad (24)$$

In the CM-frame, $\hat{s} = s = (E_1 + E_2)^2$. If, $m_3 = m_4$ and $m_1 = m_2$ with $E_1 = E_2 = E_3 = E_4 = E$, we have

$$t = -(\vec{p}_1 - \vec{p}_3)^2 = -\vec{p}_1^2 - \vec{p}_3^2 + 2\vec{p}_1 \cdot \vec{p}_3 \quad (25)$$

where $\vec{p}_1^2 = E^2 - m_1^2$ and $\vec{p}_3^2 = E^2 - m_3^2$.

So, in terms of s , t could be written as

$$t = -2s + (m_1^2 + m_3^2) + 2\sqrt{(s/4 - m_1^2)(s/4 - m_3^2)} \cos \theta, \quad (26)$$

with θ the scattering angle in the CM-frame.